Available online at www.sciencedirect.com
SCIENCE DIRECT
Biochemical and Biophysical Research Communications 343 (2006) 334–344
BBRC
www.elsevier.com/locate/ybbrc

PIN-bodies: A new class of antibody-like proteins with CD4 specificity derived from the protein inhibitor of neuronal nitric oxide synthase ☆

Cédric Bès [a,*], Samuel Troadec [a], Myriam Chentouf [a], Hélène Breton [a], Anne Dominique Lajoix [a], Frédéric Heitz [b], René Gross [a], Andreas Plückthun [c], Thierry Chardès [a]

[a] CNRS UMR 5160, Centre de Pharmacologie et Biotechnologie pour la Santé, Faculté de Pharmacie, 15 Avenue Charles Flahault, BP 14491, 34093 Montpellier Cedex 5, France
[b] CNRS UPR 1086, Centre de Recherche en Biochimie Macromoléculaire, 1919 Route de Mende, 34293 Montpellier Cedex 5, France
[c] University of Zürich, Department of Biochemistry, Winterthurerstrasse 190, 8057 Zürich, Switzerland

Received 13 January 2006
Available online 2 March 2006

Abstract

By inserting the CB1 paratope-derived peptide (PDP) from the anti-CD4 13B8.2 antibody binding pocket into each of the three exposed loops of the protein inhibitor of neuronal nitric oxide synthase (PIN), we have combined the anti-CD4 specificity of the selected PDP with the stability, ease of expression/purification, and the known molecular architecture of the phylogenetically well-conserved PIN scaffold protein. Such "PIN-bodies" were able to bind CD4 with a better affinity and specificity than the soluble PDP; additionally, in competitive ELISA experiments, CD4-specific PIN-bodies were more potent inhibitors of the binding of the parental recombinant antibody 13B8.2 to CD4 than the soluble PDP. The efficiency of CD4-specific CB1-inserted PIN-bodies was confirmed in biological assays where these constructs showed higher potencies to block antigen presentation by inhibition of IL-2 secretion and to inhibit the one-way and two-way mixed lymphocyte reactions, compared with soluble anti-CD4 PDP CB1. Insertion of the PDP into the first exposed loop (position 33/34) of PIN appeared to be the most promising scaffold. Taken together, our findings demonstrate that the PIN molecule is a suitable scaffold to expose new peptide loops and generate small artificial ligand-binding products with defined specificities.

Keywords: Scaffold protein; CD4; Protein inhibitor of neuronal nitric oxide synthase; Ligand binding; Paratope-derived peptide; Antibody

Creating small novel ligands with defined target specificity and biological properties which can mimic antibodies is one major goal of protein engineering. We and others have demonstrated that peptides derived from the antibody binding pocket, known as paratope-derived peptides (PDP), can achieve such objectives but also possess limitations [1]. The PDPs show considerable conformational flexibility in solution so that the entropic penalty upon binding is high, usually leading to significantly reduced affinities. Furthermore, their low proteolytic stability prevents or limits their use in biological assays and consequently in therapy [2,3]. To overcome such problems, one can chemically modify the PDPs through C-terminal amidation and N-terminal acetylation [4] or reduction of peptide bonds [5,6]. PDPs can be synthesized as retro-inverso peptides [7] or by using D-residues [8]. The flexibility and stability of peptides can also be restricted by grafting them onto a rigid scaffold

☆ *Abbreviations:* PIN, protein inhibitor of neuronal nitric oxide synthase; NO, nitric oxide; CDR, complementary-determining region; mAb, monoclonal antibody; H, variable region of the heavy chain; L, variable region of the light chain; PCR, polymerase chain reaction; ELISA, enzyme-linked immunosorbent assay; PDP, paratope-derived peptide; sCD4, soluble CD4; PBL, peripheral blood lymphocytes; MLR, mixed lymphocyte reaction; IL-2, interleukin-2.

* Corresponding author. Fax: +33 467 548 610.
E-mail address: cedric.bes@cpbs.univ-montp1.fr (C. Bès).

0006-291X/$ - see front matter © 2006 Elsevier Inc. All rights reserved.
doi:10.1016/j.bbrc.2006.02.126

protein. Ideally, scaffold proteins should display several features like a phylogenetically well-conserved sequence among species in order to prevent or limit immunogenicity, or a robust architecture with a well-known three-dimensional molecular organization (crystallography or NMR available), a small size, no or only a low degree of post-translational modifications, and the fusion protein should be easily produced, expressed, and purified. More importantly, the scaffold protein must contain regions that can be extensively reshaped by residue insertion or deletion without affecting its overall folding and stability properties. Various scaffold proteins have been proposed up to date but none of them retains all the above properties [9].

The protein inhibitor of neuronal nitric oxide synthase (PIN) is a highly conserved protein of 89 amino acids, displaying 90% sequence identity between *Chlamydomonas*, *Caenorhabditis elegans*, *Drosophila*, and humans. PIN was originally identified as one of the light chains of flagellar and cytoplasmic dyneins and subsequently named LC8 (light chain of 8 kDa) [10,11]. PIN was also found to be a light chain for the unconventional myosin V [12,13]. Besides its involvement in two molecular motors, PIN was also demonstrated to interact with the N-terminal region of neuronal NO synthase (nNOS), thereby inhibiting nNOS dimerization and subsequent NO production [14]. A PIN protein from human origin, C-terminally tagged with a 6-histidine sequence, was successfully affinity purified from *Escherichia coli* transformed with the pET21b-PIN plasmid in our laboratory [15]. PIN is composed of a central C-terminal β sheet containing four anti-parallel β strands (β1, β4, β5, and β2) and two N-terminal antiparallel α helices (α1 and α2) on one side and a protruding β strand (β3) on the other side, as determined by NMR spectroscopy and X-ray crystallography [16–18]. The loop connecting the α1 and α2 helices (residues 30–35) and the two turns between the β2 and β3 strands (residues 60–62) and the β4 and β5 strands (residues 78–80) protrude on the same face outside the molecule and offer an interesting starting point for inserting PDPs of defined specificity.

The transmembrane glycoprotein CD4 is a major molecular partner in the immunological synapse which leads to the optimal activation of T lymphocytes during the immune response [19]. CD4 also serves as the primary receptor for the human immunodeficiency virus (HIV), thereby allowing the virus to enter cells [20]. The anti-CD4 chimeric recombinant antibody 13B8.2 was previously expressed in the baculovirus/insect cell system. We demonstrated in vitro that this antibody inhibited T lymphocyte IL-2 secretion [21] following antigen presentation and also prevents HIV transcription in $CD4^+$ cells at a post-gp120 binding step [21–23]. From this antibody, we have developed the concept of paratope-derived peptides (PDPs), corresponding to short amino acid sequences derived from antibody variable regions [2,24–26] which are screened from a systematic exploration of antibody variable domain sequences by the Spot method [27,28]. We then demonstrated that the bioactive PDP CB1, derived from the CDR1-H region of the anti-CD4 13B8.2 mAb, displayed biological properties similar to those of the parental 13B8.2 mAb but with the intrinsic limitations of peptides when used in biological assays [2]. Within the CB1 sequence, LTTFGVHWVRQS, alanine scanning revealed that Phe, His, Trp, and Arg residues mainly contribute to its binding to CD4 [29].

In the work described in the present paper, we developed novel ligand-binding molecules, the so-called "PIN-bodies," with defined specificity, by using PIN as a scaffold protein for anti-CD4 PDP CB1 selected from the antigen-binding pocket of 13B8.2 mAb. In this initial trial, we describe the design, construction, purification, and biological characterization of these PIN-bodies. We then demonstrated that CB1-inserted PIN-bodies bind CD4 more efficiently than soluble PDP CB1. This increased binding was found to be correlated with an increased ability to block antigen presentation by inhibition of IL-2 secretion and to inhibit the one-way and two-way mixed lymphocyte reactions.

Materials and methods

Construction of PIN-bodies. DNA handling and bacterial transformations were performed according to standard procedures, unless otherwise stated. The nucleotide sequence of PDP CB1 was inserted into the PIN gene by a two-step overlapping PCR [30], using 10 pmol of the appropriate oligonucleotide pair (see description in Fig. 1B), 0.5 U of *Tfl* polymerase (Epicentre, Madison, WI), 2 mM dNTP (Invitrogen, Paisley, UK), 37.5 mM $MgCl_2$ (Epicentre), 1× Tfl buffer, and the pET21b plasmid containing the human PIN gene as the DNA matrix [15]. The PCR procedure included a 5-min denaturation step at 94 °C followed by 25 cycles at 94 °C for 30 s, 50 °C for 30 s, and 72 °C for 1 min, and ended by a 10-min elongation step at 72 °C. PCR products were run on a 1% (w/v) agarose gel and purified using the QIAquick gel extraction kit and protocol (Qiagen, Hilden, Germany). After digestion with *Nde*I and *Xho*I restriction enzymes, CB1-inserted PIN genes were ligated into the pET21a plasmid, thereby introducing a C-terminal 6-His tag (Novagen VWR International SAS, Fontenay-sous-Bois, France), using 400 U T4 DNA ligase (Promega, Madison, WI) and associated reaction buffer for 18 h at 16 °C. Ligation products were electroporated into TOP10 competent *E. coli* cells (Invitrogen), and the transformed bacteria were plated on LB plates supplemented with 50 μg/ml of ampicillin (LB-amp) and cultured for 18 h at 37 °C. The resulting clones were further screened by PCR amplification of the complete fusion gene as described above. Positive clones, bearing the CB1 sequence inserted between nucleotides coding for PIN residues N33 and I34, R60 and N61, or G79 and Q80, were sequence controlled by the dideoxynucleotide termination sequencing method. For control constructions, a peptide corresponding to the CDR2-L of 13B8.2 variable light chain (LVHDAKTLAEGV) and showing no CD4 reactivity [2] was inserted between the same positions.

Escherichia coli expression of PIN-bodies. BL21(DE3) *E. coli* cells (Invitrogen) were transformed by heat shock with the plasmid preparation from each selected clone and plate-cultured on LB-amp plates for 18 h at 37 °C. Colonies were scrapped by flooding the plates with LB medium and further cultured in 1 L of LB-amp medium at 37 °C under shaking until an A_{600} of 0.5–0.6 was reached (typically in 2–3 h). Expression of PIN-bodies was induced by adding IPTG (Euromedex, Mundolsheim, France) to a final concentration of 1 mM and performed for 18 h at 30 °C. Then, bacteria cells were harvested by centrifugation at 3000*g* for 15 min and subjected to five freeze-thaw cycles. Bacterial pellets were further suspended in sonicating buffer A [20 mM Na_2HPO_4 (pH 6.5), 0.1% Triton X-100, 1 mM $MgCl_2$, 20 mM imidazole, 10% glycerol, 10 mM β-mercaptoethanol] and sonicated twice for 30 s on ice. A protease inhibitor cocktail (Roche, Indianapolis, IN), a 1 mg/ml lysozyme solution, and DNase I were then

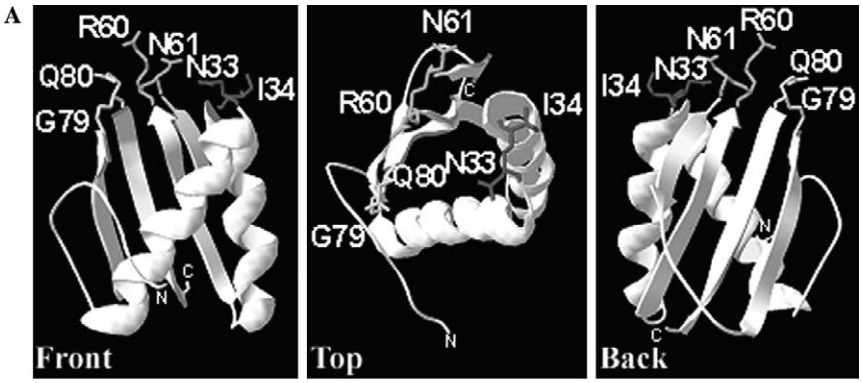

B

Name	Séquence
33/34 CB1-5'	5'-tttggtgtacactgggttcgccagtctatagagaaggatatc
33/34 CB1-3'	5'-aacccagtgtacaccaaaggtagttaagttgtacttctccaa
60/61 CB1-5'	5'-tttggtgtacactgggttcgccactctaacttcggtagctac
60/61 CB1-3'	5'-aacccagtgtacaccaaaggtagttaaccggcccacgatgca
79/80 CB1-5'	5'-tttggtgtacactgggttcgccagtctcaggtggccattctc
79/80 CB1-3'	5'-aacccagtgtacaccaaaggtagttaaacccaggtagaagta
33/34 CDR2-5'	5'-gatgcaaaaaccttagcagaaggtgtgatagagaaggatatc
33/34 CDR2-3'	5'-tgctaaggtttttgcgtcatggaccaggtgtacttctccaa
60/61 CDR2-5'	5'-gatgcaaaaaccttagcagaaggtgtgaacttcggtagctac
60/61 CDR2-3'	5'-tgctaaggtttttgcatcatggaccagccggcccacgatgca
79/80 CDR2-5'	5'-gatgcaaaaaccttagcagaaggtgtgcaggtggccattctc
79/80 CDR2-3'	5'-tgctaaggtttttgcatcatggaccagacccaggtcgaagta
T7pro-5'	5'-ttaatacgactcactatagggaattgtgagcggat
T7ter-3'	5'-ccccaaggggttatgctagttattgctcagcggtgg

C

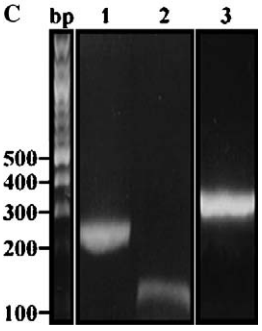

Fig. 1. Genetic construction of PIN-bodies. (A) Ribbon diagram of the structure of PIN (PDB code 1CMI) in three different projections. The PIN residues, between which the anti-CD4 CB1 peptide sequence derived from the CDR1-H region of 13B8.2 antibody was inserted, are indicated for the construction of CB1 PIN-bodies 33/34 between residues N33 and I34, 60/61 between residues R60 and N61, and 79/80 between residues G79 and Q80. The structure was adjusted by using the swiss-PDB viewer 3.7b2 software available at www.expasy.ch/spdbv. (B) Nucleotide sequences of the primers used for the construction of CB1-inserted or control peptide CDR2-inserted PIN-bodies 33/34, 60/61, and 79/80. (C) PCR amplification of 5′—(lane 1), 3′—(lane 2), and overlapping—(lane 3) PCR products for the construction of CB1-inserted PIN-body 79/80. The PCRs were fractionated on a 1% agarose gel. DNA ladder marker is annotated on the left.

added to the sonicated suspension and incubated for 20 min on ice. A second sonication step was performed before the bacterial lysate was centrifuged at 20,000*g* for 30 min at 4 °C. The PIN-bodies were recovered in the supernatant following centrifugation at 20,000*g* for 30 min at 4 °C.

Nickel-affinity and ion-exchange purification of PIN-bodies. PIN-bodies were batch-incubated for 18 h at 4 °C under orbital shaking with 3 ml of Ni–NTA superflow matrix (Qiagen), previously equilibrated with 5 volumes of buffer A. The resulting batch preparation was loaded into a column plugged onto the Biologic-LP purification system (Bio-Rad, Hercules, CA). Washings and elution were performed at 0.5 ml/min; protein concentration and conductivity were monitored during the purification processes. Washes consisted of a 10-column volume step of buffer A, followed by a 10-column volume high salt washing step with buffer A supplemented with 500 mM NaCl, and followed by an additional 10-column volume washing with buffer A to remove any traces of salts. Elution of PIN-bodies was performed with a 30-column volume gradient of imidazole from 20 to 500 mM in the same buffer A and 1-ml fractions were collected. Fractions showing the highest protein concentrations eluted between 180 and 210 mM imidazole were pooled, and directly submitted to cation-exchange purification by batch-incubation for 18 h at 4 °C under orbital shaking with 3 ml of CM sephadex C-25 resin (Sigma–Aldrich), previously equilibrated in buffer A. The resulting batch preparation was loaded into a column plugged onto a Biologic-LP purification system (Bio-Rad). Washings and elution were performed at 0.5 ml/min, protein concentration and conductivity were monitored during the purification processes. Washes consisted of a 10-column volume step of buffer A followed by a 10-column volume gradient step of NaCl from 0 to 100 mM. Elution of PIN-bodies was performed with a 30-column volume gradient of NaCl from 100 mM to 1 M and 1-ml fractions were collected. Fractions containing proteins were electrophoresed on a 13% Tricine gel. Positive fractions, showing a 9-kDa band corresponding to the PIN protein after silver-staining revelation (Amersham Pharmacia Biotech, Piscataway, NJ), were pooled, and extensively dialyzed against working buffer [20 mM Tris; 150 mM NaCl (pH 8.0)].

Characterization of PIN-bodies. Purified PIN-bodies were tested either by SDS–PAGE silver-staining following electrophoresis or by immunoblotting. After electrophoresis on a 13% Tricine gel and transfer onto a nitrocellulose membrane (Schleider and Schuell, Dassel, Germany), 6× His tag reactivity was detected by a 1:1000 peroxidase-conjugated anti-6×His-specific mAb (Sigma–Aldrich, St. Louis, MI) solution and subsequent revelation using the ECL detection system (Amersham Pharmacia).

PIN specificity of the PIN-bodies was confirmed by ELISA measurement. Different concentrations of purified PIN-bodies and wild type-PIN (WT-PIN) were coated onto microtiter plate wells (Nunc, Paisley, UK) in 100 mM $NaHCO_3$ buffer (pH 9.6), for 18 h at 4 °C. Plates were washed three times with 0.05% Tween 20 in 160 mM PBS (pH 7.2) (washing buffer, PBS-T) and blocked with 1% non-fat powdered milk in PBS-T (PBS-T-1%M) for 1 h at 37 °C. After three washings, anti-PIN mAb (BD transduction Laboratories, Lexington, KY) at a 1:1250 dilution in PBS-T-1%M was added and incubated for 2 h at 37 °C. After three washings, a peroxidase-conjugated anti-mouse IgG whole molecule (Sigma–Aldrich) at a 1:1000 dilution in PBS-T-1%M was added for 1 h at 37 °C. After three washings and subsequent addition of peroxidase substrate, absorbance was measured at 490 nm.

Biophysical characterization of PIN-bodies was first performed by measuring far-UV CD spectra with a Jasco J-810 spectropolarimeter (Tokyo, Japan) at 20 °C in working buffer (see above). The spectra represent an average of two scans recorded at a speed of 20 nm/min and a resolution of 0.1 nm. PIN-body concentration was 0.3 mg/ml. A cell with a 0.1-cm optical path length was used. Chemical denaturation studies were performed to compare unfolding transitions of PIN-bodies by measuring changes in far-UV CD spectra following the above experimental conditions. PIN-bodies were diluted to a final concentration of 0.3 mg/ml in ultrapure guanidinium–hydrochloride (Euromedex, Mundolsheim, France) solutions

ranging from 0 to 3 M in working buffer and allowed to come to equilibrium by incubating the samples at 25 °C for 18 h. Unfolding of PIN-bodies was monitored at 222 nm upon denaturant concentration.

Soluble peptide synthesis. PDP CB1 (see sequence in introduction) derived from the 13B8.2 CDR1-H region and irrelevant PDP CB4 (WRSGITDYNVPF) derived from the CDR2-H and showing no CD4 reactivity in a soluble form [2], both with Lys-Cys residues added to both the C- and N-termini, were synthesized by Fmoc solid-phase synthesis on an AMS422 robot (Abimed, Langenfeld, Germany), cyclized, and purified as described previously [25]. Both peptides showed homogeneity in high performance liquid chromatography at the expected monomeric molecular weight and were resuspended into deionized water.

ELISA measurement of PIN-bodies and WT-PIN binding to CD4. A 2 nM solution of purified sCD4 (Perkin-Elmer, Boston, MA) in PBS was coated for 18 h at 4 °C onto 96-well microtiter plates (Nunc). Four washes with PBS-T were performed before and after blocking the plates with PBS-T-1%M for 1 h at 37 °C. Thereafter, 100 µl of 2-fold serial dilutions of PIN-body preparations at an initial concentration of 2.5 µM was added to each well and incubated for 2 h at 37 °C. WT-PIN was used as a negative control. Following four washes in PBS-T, bound 6×His-tagged PIN-bodies were detected by addition of 100 µl of a 1:1000 solution of peroxidase-conjugated anti-6×His mAb (Sigma–Aldrich) for 1 h at 37 °C, followed by four washings with PBS-T and subsequent addition of peroxidase substrate. Absorbance was measured at 490 nm.

Sandwich ELISA measurement of CD4 binding to CB1-inserted PIN-bodies compared to soluble PDP CB1. Three replicates corresponding to 2-fold serial dilutions of CB1-inserted PIN-bodies or soluble PDP CB1 at an initial concentration of 2.5 or 100 µM, respectively, were coated for 18 h at 4 °C in 100 mM $NaHCO_3$ buffer (pH 9.6) onto 96-well microtiter plates. CDR2-L-inserted PIN-bodies, soluble PDP CB4, and WT-PIN were used as negative controls. Four washes with PBS-T were performed before and after blocking the plates with PBS-T-1%M for 1 h at 37 °C. A 10 nM solution of sCD4 (Perkin-Elmer) was added to each well and the plates were incubated for 2 h at 37 °C. Following four washes in PBS-T, sCD4 binding to PIN-bodies or peptides was evidenced by adding a 1:2000 solution of a goat anti-CD4 polyclonal antibody (RD Systems, Minneapolis, MI) and incubated for 2 h at 37 °C. Four washes with PBS-T were performed before and after the addition of a 1:5000 solution of peroxidase-conjugated mouse anti-goat IgG (Jackson Immunoresearch, West Grove, PA); peroxidase activity was detected by adding the substrate and then measuring the absorbance at 490 nm.

ELISA inhibition of recombinant Fab 13B8.2 binding to CD4 by CB1-inserted PIN-bodies compared to soluble PDP CB1. A 2 nM solution of purified sCD4 (Perkin-Elmer) in PBS was coated for 18 h at 4 °C onto 96-well microtiter plates (Nunc). Four washes with PBS-T were performed before and after blocking the plates with PBS-T-1%M for 1 h at 37 °C. Thereafter, 50 µl of 2-fold serial dilutions of CB1-inserted PIN-bodies or soluble PDP CB1 at an initial concentration of 5 µM or 200 µM, respectively, was co-incubated with 50 µl of a 400 nM solution of recombinant 13B8.2 Fab for 2 h at 37 °C under orbital shaking at 150 rpm. WT-PIN or irrelevant PDP CB4 were used as negative controls. After four washings with PBS-T, residual bound 13B8.2 Fab was detected by adding 100 µl per well of a 1:1000 solution of peroxidase-conjugated anti-human kappa chain mAb (Sigma–Aldrich) for 1 h at 37 °C, followed by four washings with PBS-T and subsequent addition of peroxidase substrate. Absorbance was measured at 490 nm.

IL-2 secretion assay following antigen presentation. EBV-Lu antigen-presenting cells (10^6 cells/ml), previously pulsed overnight with a 75-µM solution of the pep24 stimulator peptide derived from HIV gp120 [31], were co-cultured with pdb10f responder T cells (4×10^5 cells/ml) in the presence or absence of PIN-bodies or PDPs for 24 h. Thereafter, 100 µl of the culture supernatant was harvested and tested for IL-2 secretion using an ELISA commercial kit and protocol (Pharmingen, San Diego, CA). A positive control for IL-2 secretion was performed as described above except that the pdb10f responder cells were activated with a 0.6-nM solution of a murine anti-CD3 mAb (Pharmingen).

One-way and two-way mixed lymphocyte reactions. Human PBLs were purified by Histopaque (Sigma) density centrifugation from blood samples of healthy donors obtained at the Etablissement Français du Sang (EFS, Montpellier, France). In a one-way MLR experiment, stimulator PBLs from donor A, diluted at 1×10^6 cells/ml in RPMI medium supplemented with 10% foetal calf serum and antibiotics, were treated with mitomycin C (Calbiochem VWR International SAS, Fontenay-sous-Bois, France) for 30 min at 37 °C. After washings, 1×10^5 cells/well of mitomycin C-treated PBLs were co-incubated with 1×10^5 cells/well of untreated responder PBLs from an unrelated donor B in the presence or absence of various concentration of PIN-bodies and cultured for 5 days at 37 °C in a 5% CO_2 incubator. In a two-way MLR, similar experimental procedure was used except that PBLs from donor A were not treated with mitomycin C. Various controls were performed in one- and two-way MLR (see legend in Figs. 6 and 7). In both cases, proliferation of responder cells was measured by incorporation of a 1:100 dilution of bromodesoxyluridine (BrdU) during the last 18 h of cell culture. Incorporated BrdU was detected by using the cell proliferation ELISA BrdU commercial kit and protocol (Roche).

Results

Design and construction of the PIN-bodies

Using the crystal structure of PIN as a guide (Fig. 1A), we decided to introduce the PDP CB1 sequence between nucleotides encoding residues N33 and I34, located in the loop connecting the α1 and α2 helices and between residue pairs R60/N61 and G79/Q80, corresponding to the two turns between the β2 and β3 strands and the β4 and β5 strands, respectively. These residues protrude on the same face outside the molecule (Fig. 1A). The starting point for PIN-body construction was the pET21b-PIN plasmid [15], which bears the human PIN sequence and was used as template for PCR mutagenesis. A two-step overlapping extension PCR was performed with appropriate oligonucleotides (Fig. 1B) [30]. First, the 5′- and 3′-products of the PIN-bodies bearing the CB1 sequence inserted at the designed position were prepared as exemplified by amplifications of a 250-bp 5′-product (between T7pro5′ and 79/80CB1-5′ oligonucleotide pair) and a 95-bp 3′-product (between 79/80CB1-3′ and T7ter3′ oligonucleotide pair) for the CB1-inserted PIN-body 79/80 (Fig. 1C). The second step of the PCR was performed by assembling the two 5′- and 3′-products by using T7pro-5′ and T7ter-3′ oligonucleotide pairs resulting in a full-length genetically modified human PIN gene bearing the CB1 sequence inserted between nucleotides encoding residues G79 and Q80 of the PIN sequence, as demonstrated in Fig. 1C.

The 6×histidine-tagged PIN-bodies as well as the WT-PIN were produced as soluble proteins in *E. coli* strain BL21(DE3) and purified according to a two-step procedure including a Ni^{2+}–NTA affinity column, followed by cation-exchange purification leading to the obtention of highly pure and concentrated recombinant proteins. Yields of production ranged from 30 to 45 mg/L of *E. coli* culture at an OD 600 nm of 10. Silver-staining revelation of the highly purified products only showed a major 9 kDa-band, corresponding to the expected size of PIN, together with a minor 18 kDa-band, probably being the already observed dimeric form (Fig. 2A) [15]. The PIN dimer was only visualized in WT-PIN, CB1- and control peptide

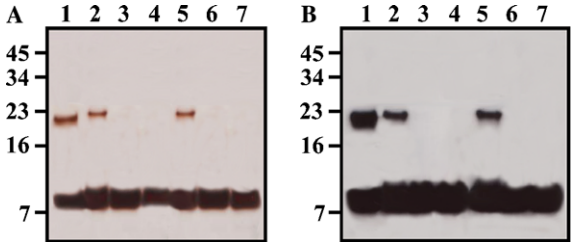

Fig. 2. Production and characterization of PIN-bodies following the two-step purification procedure. (A) Silver-staining of a 13% Tricine SDS–PAGE gel of electrophoresed PIN-body preparations. (B) Western blot analysis of purified PIN fractions detected by peroxidase-conjugated anti-histidine antibody and revealed by electrochemoluminescence. In both cases, lane 1 corresponds to WT-PIN, lanes 2–4 correspond to CB1-inserted PIN-bodies 33/34, 60/61, and 79/80, respectively, and lanes 5–7 correspond to control peptide CDR2-inserted PIN-bodies 33/34, 60/61, and 79/80, respectively.

CDR2-inserted PIN-body 33/34 preparations, even if the dimerization seemed to be a little less efficient for the PDP-inserted PIN-bodies than for WT-PIN. In a peroxidase-conjugated anti-6×His mAb Western-blotting experiment (Fig. 2B), both monomeric and dimeric bands were recognized, obviously demonstrating that the higher band is most likely the dimeric form.

Biophysical characterization of PIN-bodies

All the purified PIN constructions, either WT- or PDP-inserted ones, showed similar and dose-dependent binding to an anti-PIN mAb, as demonstrated by ELISA (Fig. 3); such an observation suggests that the overall PIN conformation was not globally altered by the PDP insertion.

Further biophysical characterization of the PIN-bodies was performed to confirm these initial ELISA observations. Far-UV CD spectra were recorded for all PIN-bodies; and as exemplified in Fig. 4A for CB1-inserted PIN-bodies and control peptide CDR2-inserted PIN-body 33/34, a similar spectrum to that of WT-PIN was obtained for all constructs. The negative peak observed at 222 nm and the shoulder around 210 nm being probably representative of the β sheet and α helix secondary structure components of the PIN protein.

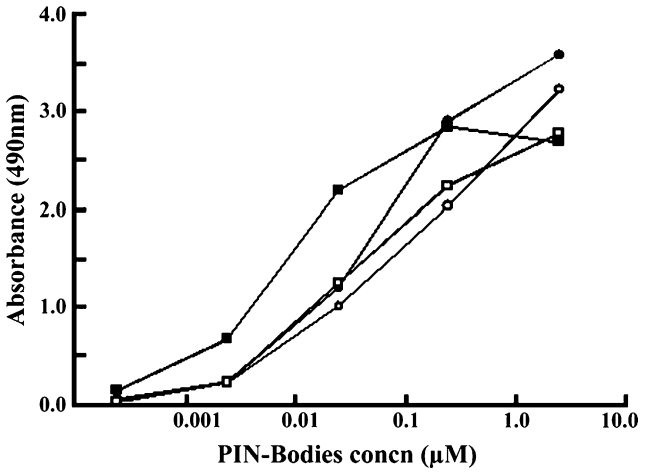

Fig. 3. Anti-PIN ELISA measurement for WT-PIN (■), CB1-inserted PIN-bodies 33/34 (○), 60/61 (●), and 79/80 (□). Each value represents the mean of triplicate determinations.

Resistance of the PIN-bodies to guanidinium–hydrochloride unfolding was then analyzed. The unfolding transition was monitored by titrating the changes measured in the far-UV CD spectra as a function of denaturant concentration as exemplified for WT-PIN denaturation (Fig. 4B). As exemplified in Fig. 4C for CB1- and the control peptide CDR2-inserted PIN-bodies 33/34, when plotting the molar ellipticity obtained for the negative peak observed at 222 nm upon denaturant concentration, similar transitions to that of WT-PIN were obtained for all constructs with a mid-point for unfolding around 0.5 M of guanidinium–hydrochloride. This transition was fully reversible upon dilution back through the curve to zero denaturant concentration (data not shown). Taken together, these data indicate that the overall conformation and stability/folding properties of the PIN-bodies compared with those of WT-PIN were not affected by any of the peptide insertions.

CB1-inserted PIN-bodies bind more efficiently CD4 than soluble PDP CB1

A dose-dependent binding of CB1-inserted PIN-bodies 33/34, 60/61, and 79/80 to CD4 was demonstrated by ELISA (Fig. 5A), whereas WT-PIN does not bind to CD4. In a similar manner, control peptide CDR2-inserted PIN-bodies 33/34, 60/61, and 79/80 showed no binding to CD4 (data not shown). The CD4 binding curves indicated stronger binding for CB1-inserted PIN-body 33/34 than for CB1-inserted PIN-bodies 60/61 and 79/80 (Fig. 5A), suggesting that insertion between positions N33 and I34 would be the best way to insert this peptide, and conceivably other peptides of defined antigen specificity as well.

As demonstrated in a sandwich ELISA with immobilized PIN-bodies or peptides and soluble sCD4 at 10 nM which gets detected by anti-CD4 polyclonal antibody (Fig. 5B), 2.5 μM of CB1-inserted PIN-bodies 33/34, 60/61, and 79/80 significantly bound CD4, but with a greater CD4 binding capacity for PIN-body 33/34 than for PIN-body 60/61 or 79/80; this binding was dose-dependent in the 0.1–2.5 μM concentration range of constructs. On the other hand, significantly lower CD4 binding to soluble PDP CB1 was observed in the 6.25–100 μM concentration range (Fig. 5B). In each case, no CD4 binding was observed for WT-PIN or for the control PDP CB4 in the same concentration ranges. It should be pointed out however that due to the coating step conditions this is not clear how much of the soluble or inserted CB1 peptides could be immobilized, and whether the immobilization could further constrain their conformations such that binding is impeded.

Because of the uncertainties of peptide immobilization, the higher CD4 binding capacity of CB1-inserted PIN-bodies in comparison to that of soluble CB1 was indirectly

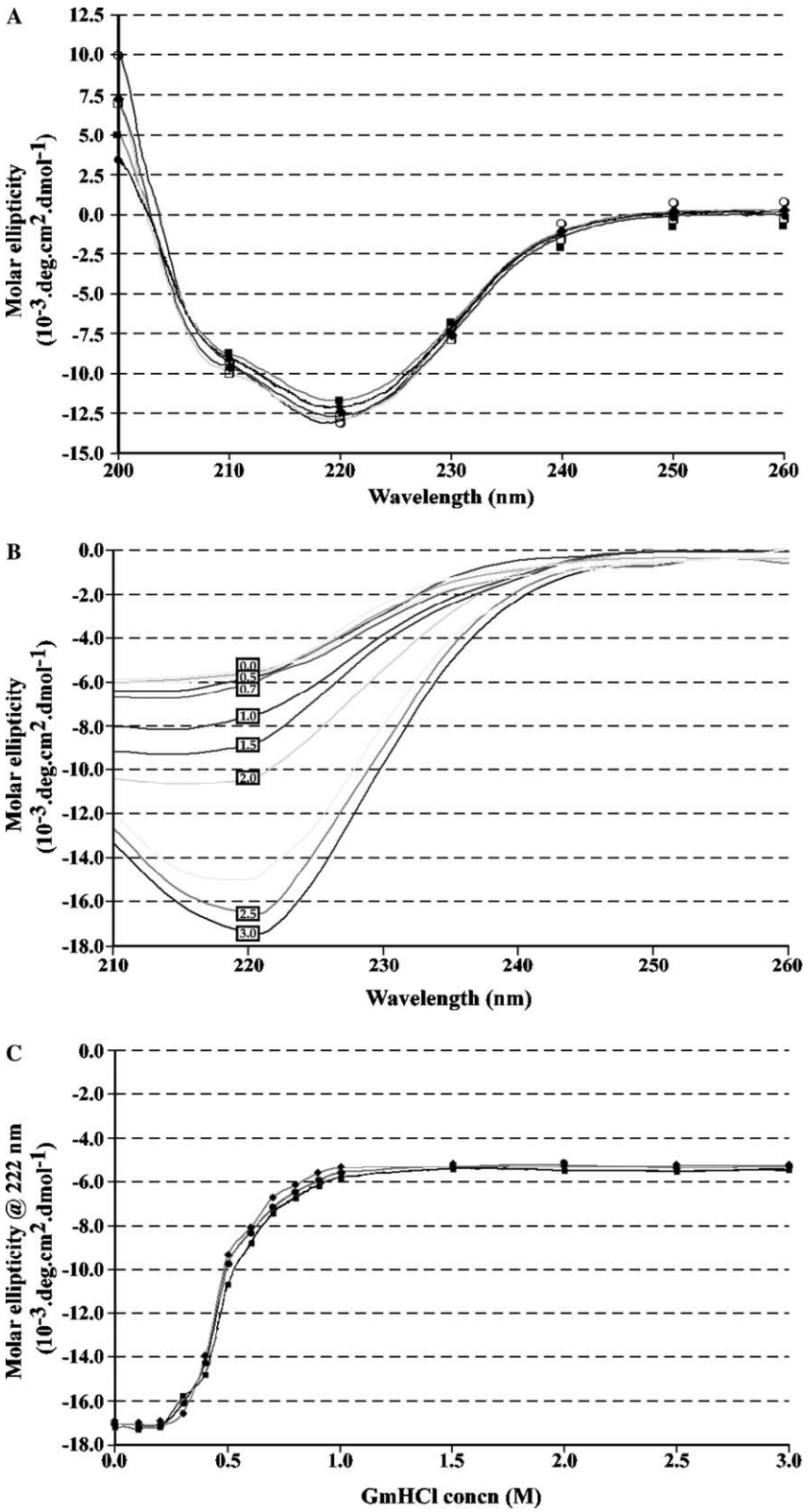

Fig. 4. Biophysical characterization of PIN-bodies. (A) Far-UV CD spectra of CB1-inserted PIN-bodies 33/34 (■), 60/61 (○), 79/80 (□), and control peptide CDR2-inserted PIN-body 33/34 (♦) vs WT-PIN (●). (B) Far-UV CD spectra of guanidinium–hydrochloride unfolding titrations of WT-PIN; inset, the range of 0–3 M of GmHCl. (C) Molar ellipticity measured at 222 nm from far-UV CD spectra of guanidinium–hydrochloride unfolding titrations of WT-PIN (●), CB1-inserted PIN-body 33/34 (■), and control peptide CDR2-inserted PIN-body 33/34 (♦) in a range of 0–3 M of GmHCl. In all cases, displayed data represent the most typical result obtained in three unfolding experiments using three independent protein preparations.

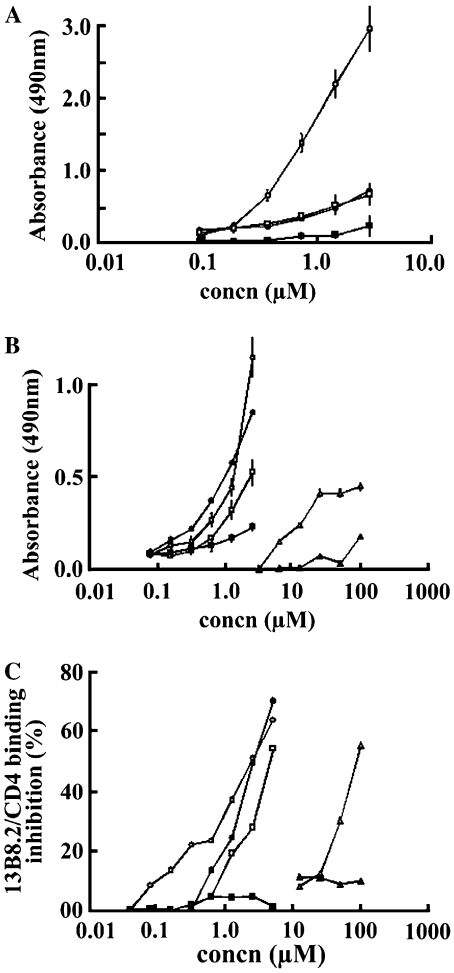

Fig. 5. CD4 binding studies of CB1-inserted PIN-bodies in comparison with soluble PDP CB1. (A) CD4 binding of various concentrations of CB1-inserted PIN-bodies 33/34 (○), 60/61 (●), and 79/80 (□) in comparison with WT-PIN (■). (B) Sandwich ELISA binding of various concentrations of plastic-coated CB1-inserted PIN-bodies 33/34 (○), 60/61 (●), and 79/80 (□) in comparison with PDP CB1 (Δ) to soluble CD4. (C) ELISA inhibition of CD4 binding to recombinant anti-CD4 Fab 13B8.2 by various concentrations of CB1-inserted PIN-bodies 33/34 (○), 60/61 (●), and 79/80 (□) in comparison with PDP CB1 (Δ). Mean absorbance at 450 nm varied from 0.027 with medium alone to 1.35 for CD4 binding to Fab 13B8.2 without inhibitor. In all formats, each value represents the mean ± SD of triplicate determinations; in the two last formats, WT-PIN (■) and irrelevant PDP CB4 (▲) were used as negative controls.

confirmed by ELISA inhibition (Fig. 5C). In this case, approximately 1 μM of CB1-inserted PIN-bodies inhibited 50% of the binding of 200 nM recombinant Fab 13B8.2 to CD4. Binding inhibition occurred in the 0.1–5 μM concentration range of CB1-inserted PIN-bodies; CB1-inserted PIN-body 33/34 showing the highest inhibition capacity with an IC_{50} of 0.8 μM. The dissociation constant K_D of recombinant Fab 13B8.2 for CD4 measured with the Biacore technology was determined as 3.3 nM [21]. Altogether, these data allowed us to calculate a K_D of 12 nM for the CB1-inserted PIN-body 33/34 interaction with the CD4 molecule [32]. As fifty percent inhibition of recombinant Fab 13B8.2 binding to CD4 was only obtained by using approximately 80 μM of soluble PDP CB1, these data clearly reflect a better anti-CD4 binding activity for the CB1 peptide when inserted into the PIN scaffold. As a control, no 13B8.2/CD4 binding inhibition was observed with WT-PIN or control soluble PDP CB4.

Anti-CD4 CB1-inserted PIN-bodies inhibit antigen presentation-induced response of T lymphocytes to peptide-pulsed presenting cells

To further investigate whether the physiological properties of CD4 could be inhibited by PIN-bodies presenting a peptide derived from a biologically active anti-CD4 antibody, it was tested whether the PIN-bodies would inhibit IL-2 secretion by T-helper lymphocytes upon contact with antigen-presenting cells [19,21]. This experiment was performed to compare the biological activities of CB1-inserted PIN-bodies with those of the soluble PDP to assess whether the scaffold strategy led to improved biological stability and so activity of the peptide when grafted onto the PIN scaffold.

In our hands, Pep24-pulsed EBV-Lu APC co-cultured with pdb10F responder T cells led to IL-2 secretion following antigen presentation, as already described [31]. As shown in Fig. 6, a 0.3–2.5 μM dose-dependent inhibition of IL-2 secretion was demonstrated following incubation with CB1-inserted PIN-bodies in this T cell activation model. At the same concentrations, control peptide CDR2-inserted PIN-bodies 33/34, 60/61, and 79/80 did not display any inhibitory activity. CB1-inserted PIN-body 33/34 was more inhibitory than CB1 PIN-bodies 60/61 and 79/80; these data correlate with the CD4-binding analyses. In this experiment, inhibition of IL-2 secretion by soluble

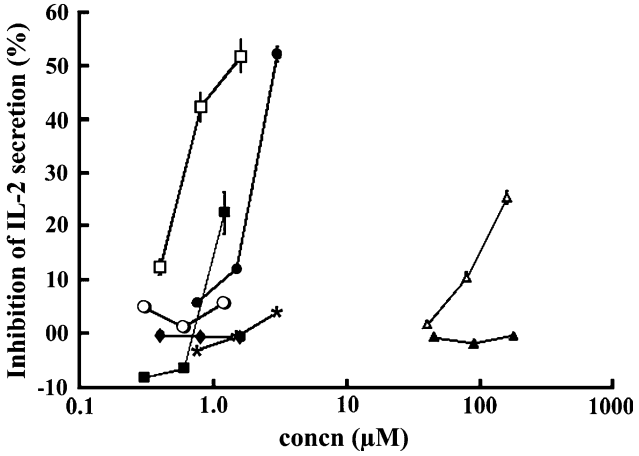

Fig. 6. Inhibition of IL2 secretion by pdb10F T cells sensitized with pep24-stimulated EBV-Lu antigen-presenting cells and co-cultured with various concentrations of CB1-inserted PIN-bodies 33/34 (□), 60/61 (●), and 79/80 (■) vs PDP CB1 (Δ). Control peptide CDR2-inserted PIN-bodies 33/34 (○), 60/61 (♦), 79/80 (*), and irrelevant PDP CB4 (▲) were used as negative controls. Mean absorbance at 450 nm varied from 0.074 for pdb10F cells co-cultured with unstimulated EBV-Lu antigen-presenting cells to 2.637 for pdb10F cells co-cultured with pep24-stimulated EBV-Lu antigen-presenting cells. Each value represents the mean ± SD of triplicate determinations.

PDP CB1 only occurred in the 50–200 μM concentration range. Soluble PDP CB1, that exhibited a CD4-binding ability 10- to 100-fold lower than that of CB1-inserted PIN-bodies, also had a lower inhibitory capacity in the antigen presentation assay.

Anti-CD4 CB1-inserted PIN-bodies block the proliferation of allogeneic-stimulated human peripheral blood lymphocytes in one-way and two-way mixed lymphocyte reactions

In contrast to the above experiment with a well-defined peptidic T cell antigen, the mixed lymphocyte reaction (MLR) tests the reaction of human T cells to foreign antigen-presenting cells, which is caused by the direct recognition of the MHC and/or presented foreign peptides in this MHC. In the "one-way" MLR, cells from the human donor A are treated with mitomycin C, a DNA alkylating agent acting as a cell proliferation inhibitor, such that proliferation of cells from human donor B can be measured selectively. In the "two-way" experiment, this mitomycin C treatment is omitted, such that APCs from both donors can stimulate the T cells of the other donor leading to a bi-directional proliferation.

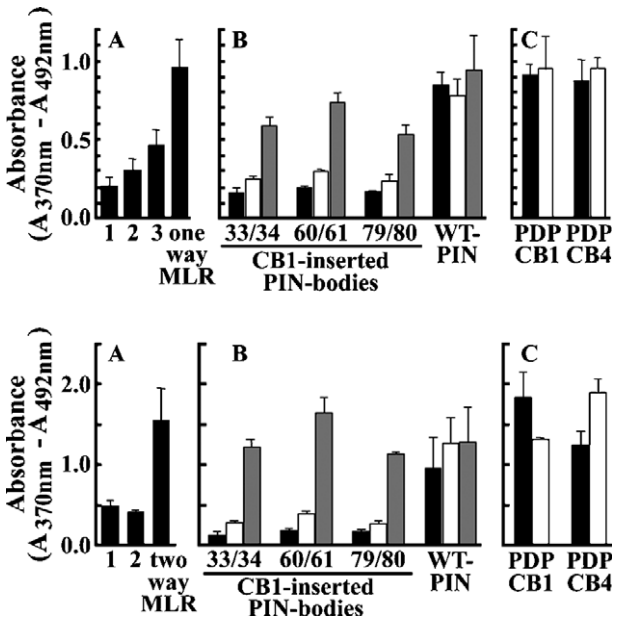

Fig. 7. Inhibition of the proliferation of allogeneic-stimulated human peripheral blood lymphocytes co-cultured with various concentrations of CB1-inserted PIN-bodies 33/34, 60/61, and 79/80 vs PDP CB1. Upper panel, one-way mixed lymphocyte reaction format inhibition of proliferation. (A) Controls for one-way MLR in the absence of inhibitor. One-way MLR corresponds to the proliferation of responder cells co-incubated with mitomycin-treated stimulator cells; control 1 corresponds to the proliferation of mitomycin-treated stimulator cells alone; control 2 corresponds to the proliferation of 1× responder cells; and control 3 corresponds to the proliferation of 2× responder cells. (B) Inhibition of one-way MLR by CB1-inserted PIN-bodies vs WT-PIN at concentrations of 2.5 μM (■), 0.25 μM (□), and 0.025 μM (▩). (C) Inhibition of one-way MLR by PDP CB1 vs irrelevant PDP CB4 at concentrations of 100 μM (■) and 10 μM (□). Lower panel, two-way mixed lymphocyte reaction format inhibition of proliferation. (A) Controls for two-way MLR in the absence of inhibitor. Two-way MLR corresponds to the proliferation of responder cells from two different donors; control 1 corresponds to the proliferation of syngeneic responder cells from the first donor alone; and control 2, corresponds to the proliferation of syngeneic responder cells from the second donor alone. (B) Inhibition of two-way MLR by CB1-inserted PIN-bodies vs WT-PIN at concentrations of 2.5 μM (■), 0.25 μM (□), and 0.025 μM (▩). (C) Inhibition of two-way MLR by PDP CB1 vs irrelevant PDP CB4 at concentrations of 100 μM (■) and 10 μM (□). In both panels, each value represents the means ± SD of three independent experiments.

In a one-way MLR experiment, PBLs from unrelated donor B were able to proliferate in response to mitomycin C-treated stimulator cells from donor A, as determined by BrdU incorporation (Fig. 7 upper panel, A, one-way MLR). In contrast, control 1, corresponding to mitomycin C-treated stimulator cells alone, control 2, corresponding to responder cells alone, and control 3, corresponding to twice the concentration of responder cells were not able to proliferate (Fig. 7 upper panel, A). Co-incubation of responder and stimulator cells with anti-CD4 CB1-inserted PIN-bodies led to a dose-dependent inhibition of one-way MLR; such inhibition occurring in the range of 0.025–2.5 μM of PIN-bodies. On the other hand, WT-PIN did not block the proliferation of allogeneic-stimulated human PBLs in a one-way MLR experiment (Fig. 7 upper panel, B). Finally, no inhibition was observed with soluble PDP CB1 or with control PDP CB4 (Fig. 7 upper panel, C).

In a two-way MLR experiment (Fig. 7 lower panel, A), bi-directional proliferation between untreated PBLs from donors A and B was observed, whereas syngeneic control 1, corresponding to responder cells from the donor A alone, and syngeneic control 2, corresponding to responder cells from the donor B alone, were not able to proliferate. Similar results of inhibition by the anti-CD4 CB1-inserted PIN-bodies were obtained in the two-way MLR (Figs. 7 lower panels, B and C) as in the one-way MLR, demonstrating a dose-dependent inhibition of anti-CD4 CB1-inserted PIN-bodies.

Discussion

Scaffold proteins have a great potential for displaying structured peptide loops with defined binding properties for use in biotechnological and biomedical applications. Various scaffold proteins have been proposed and tested, and have recently been reviewed [9,33]. In the present work, the binding loop has been directly taken from an antibody, and thus did not have to be selected from a library. The main purpose of the protein framework in an application such as the present one is to provide a well-expressing protein backbone, which is stable and keeps these properties also when a loop of interest is inserted. The scaffold protein should thus be small and compatible with bacterial expression. PIN does not possess any disulfide bonds and can thus be produced in the bacterial cytoplasm in a functional form. A phylogenetically well-conserved sequence is often a first indication of favorable

biophysical properties, and also bodes well for expecting low immunogenicity, even though the inserted peptide sequence constitutes always an uncertainty for immunogenicity in every scaffold, even human antibody variable domains [9,33]. In this initial series of experiments, we described the successful use of the protein inhibitor of neuronal nitric oxide synthase (PIN) as a scaffold for anti-CD4 paratope-derived peptides from the antigen-binding pocket [29] of the 13B8.2 antibody.

Based on the crystal structure of human PIN [16], we successfully designed, constructed, and characterized three different PIN-bodies with CD4 binding activity and CD4 inhibition-specific biological properties after insertion of the anti-CD4 PDP CB1, derived from the paratope of the biologically active 13B8.2 mAb [2]. We designed the PDP insertion into three different exposed loops that connect the α1 and α2 helices (residues 33/34), the β2 and β3 strands (residues 60/61), and the β4 and β5 strands (residues 78–80). These CB1-inserted PIN-bodies proved to be easily and reliably produced in *E. coli* as soluble recombinant proteins and could be purified to homogeneity by a two-step purification procedure, leading to highly pure and concentrated products as demonstrated by SDS–PAGE analyses. Circular dichroism and guanidinium–hydrochloride stability analyses did not show any modifications in the structure and stability of the PIN-bodies in comparison with the WT-PIN.

The PDP CB1 consists of 12 residues and is characterized by the essential residues FxxHWxR [29]. These residues must be accessible and seem to be correctly displayed in PIN-bodies, as they bind CD4 and show similar inhibitory activities as in the parental mAb. These findings suggest that the PIN scaffold allows an overall PDP conformation similar to that of the exposed CDR1-H loop of 13B8.2 antibody, from which the CB1 sequence was derived. All ELISA measurements demonstrated an increased anti-CD4 binding activity for the CB1-inserted PIN-bodies compared with the soluble PDP CB1. The dissociation constant of CB1-inserted PIN-body 33/34 to CD4 was indirectly calculated as 12 nM K_D, this value being around 4-fold lower than the parental 13B8.2 mAb but demonstrating a 10-fold improvement with regard to what we previously reported for anti-CD4 soluble PDP [25,26]. Altogether, these data probably reflect a restricted flexibility of the peptide once grafted onto the PIN scaffold, with a lower entropic penalty upon binding to the target than the soluble peptides and consequently resulting in higher affinity. Constrained peptides were previously reported to be better binders than linear ones [6,34–37]. The improved anti-CD4 binding properties of the CB1-inserted PIN-bodies compared to that of the peptide alone translated into enhanced biological effects in both the IL-2 secretion inhibition assay and the one- and two-way MLR. These findings also argue in favor of an improved protection against proteolysis which is limiting the use of soluble peptides in biological assays and consequently in therapy [2,3].

The CB1-inserted PIN-body 33/34 displayed around 100-fold higher CD4 binding efficiency than that of soluble PDP CB1 and displayed the best anti-CD4 properties among the three constructs. One explanation could be that the engineering of residues 33/34 from the 5-amino acid loop that connects the α1 and α2 helices [16] may seem to be the best way to display anti-CD4 PDP on the PIN scaffold, compared to insertions into the turns between the β2 and β3 strands (residues 60/61) or the β4 and β5 strands (residues 78–80). These turns are probably both too strained and not protruding enough to correctly display the looped PDP conformation. Nevertheless, the overall structure of these two last constructs does not seem to be affected as demonstrated by circular dichroism and guanidinium–hydrochloride stability analyses.

Another explanation for the better efficiency of CB1-inserted PIN-body 33/34 could be related to the dimerization capability of PIN. Indeed, PIN was already demonstrated to bind its target proteins as a dimer [16,18]. In the absence of any ligand, dimeric PIN is in equilibrium with its monomeric form; this equilibrium is dependent on the protein concentration, ionic force, and pH [16,38]. PIN dimerization occurs through the hydrophobic surface formed by the five β strands, thereby exposing the charged residues of the two α helices at the surface [16,18]. The core of the dimer is composed of the β3 strand (residues 62–66) of one monomer, pairing with the β2 strand (residues 54–60) of the other monomer to extend the antiparallel β sheets to five strands. Furthermore, side-chain hydrogen bonding has been reported in the PIN dimer between residues R60 and G61 [16]. We can assume that if any of these residues were mutated, for example, following construction of the PIN-bodies, the dimer interface would irreparably lose complementarity. This is consistent with the results of our silver-staining SDS–PAGE and Western-blotting experiments demonstrating that just like WT-PIN, PDP-inserted PIN-bodies 33/34 are still able to form dimers whereas PDP-inserted PIN-bodies 60/61 and 79/80 are not. However, such loss of dimer structure does not completely prevent the use of PIN regions 60/61 and 79/80 as scaffold support for the insertion of PDP of defined specificity since anti-CD4 PIN-bodies 60/61 and 79/80, as monomers, still bind to CD4 and induce biological effects, even though these effects were found to be lower than those observed for CB1-inserted PIN-body 33/34. We previously reported that the parental monoclonal 13B8.2 antibody and the derived chimeric recombinant rIgG1 [23] and Fab fragment [21] are at least 10-fold more potent in the biological activities investigated than the CB1-inserted PIN-body 33/34.

We are currently investigating two strategies to improve CB1-inserted PIN-bodies further. Target-binding and related biological activities may become improved by inserting the 12-mer PDP CB1 into the PIN scaffold, following deletion of residues 31–35 from the loop between the α1 and α2 helices, in an attempt to display PDP CB1 even more efficiently. Alternatively, by inserting PDP

CB1 at all three positions in the same PIN-body, an enhanced affinity of the resulting single construct might result from multivalent binding and/or enhanced rebinding [39,40].

The fact that the PIN structure is well conserved among various species [16] should constitute an advantage in terms of low immunogenicity when PIN-bodies would be used for injection. The small 9-kDa size of PIN-bodies could enable them to penetrate faster and better into tissues, which could be an advantage when used for imaging or drug delivery. Furthermore, the PIN scaffold is of human origin in contrast to numerous proposed scaffold structures such as murine single immunoglobulin domains [41], bovine or bacterial protease inhibitors [42,43], bacterial helix bundles [44], lipocalins from *Pieris brassicae* [45], knottins of various origins [46], scorpion toxins [47,48], and bacterial enzymes [49] reducing if necessary any potential antigenic response. The use of antibody variable light chain domains even from human origin was also reported to successfully present small peptidic sequences leading to biological active binders [50,51]. Indeed, as compared with the time-consuming and hard to perform engineering of variable domains of antibody heavy (IGHV) and light (IGL/KV) chains to function as small recognition units and to retain some of their natural or directed antigenic affinity, the PIN-body strategy does not require such sophisticated engineering.

An extension of the strategy would be not to insert a loop sequence with a known binding function (taken from a previously "selected" molecule, such as mAb) but to select binders directly from libraries. Such constrained peptide libraries could be useful not only for epitope identification, but also as binding molecules in their own right, e.g., to receptors binding peptidic or non-peptidic ligands. Therefore, our data allow us to envisage the use of the PIN scaffold as small recognition units for displaying randomized residues derived, for example, from synthetic complementarity region 3 of antibodies or even to display random peptides that may be useful for epitope identification or pharmacological ligands for G protein-coupled receptors.

In summary, the PIN molecule displays all the required properties for an ideal scaffold and can serve as a suitable scaffold for supporting ligand-binding loops with or without pre-defined specificities. Because of the favorable biophysical properties of the PIN molecule, this strategy holds promise in biotechnology for deriving molecules for pharmaceutical applications.

Acknowledgments

The skillful assistance of C. Nguyen in synthesizing the soluble peptides is acknowledged. We thank Dr. P. De Berardinis for the human lymphoblastoid B cell line EBV-Lu and the murine T cell line pdb10F. The authors are indebted to Dr S. L. Salhi for the editorial revision of the manuscript. C. B. received fellowships successively from the Agence Nationale de Recherche contre le SIDA and the Ensemble Contre le SIDA/SIDACTION. S.T. and M.C. were both recipients of fellowships from the Ligue Nationale contre le Cancer, Comité de l'Hérault. This work was supported by institutional funds from the Agence Nationale de la Recherche contre le SIDA (No. 2003/171).

References

[1] D. Laune, F. Molina, G. Ferrières, S. Villard, C. Bès, F. Rieunier, T. Chardès, C. Granier, Application of the Spot method to the identification of peptides and amino-acids from the antibody paratope that contribute to antigen binding, J. Immunol. Methods 267 (2002) 53–70.

[2] C. Bès, L. Briant-Longuet, M. Pugnière, D. Bresson, M. Cerutti, J.-C. Mani, B. Pau, P. De Berardinis, G. Devauchelle, C. Devaux, C. Granier, T. Chardès, Efficient CD4-binding and immunosuppressive properties of the 13B8.2 monoclonal antibody are displayed by its CDR-H1-derived peptide CB1, FEBS Lett. 508 (2001) 67–74.

[3] K. Hilpert, H. Wessner, J. Schneider-Mergener, K. Welfe, R. Misselwitz, H. Welfe, A.C. Hocke, S. Hippenstiel, W. Höne, Design and characterization of a hybrid miniprotein that specifically inhibits porcine pancreatic elastase, J. Biol. Chem. 278 (2003) 24986–24993.

[4] R. Hussain, N.S. Courtenay-Lucket, G. Siligardi, Structure–function correlation and biostability of antibody CDR-derived peptides as tumour imaging agents, Biomed. Pept. Proteins Nucleic Acids 2 (1996) 67–70.

[5] N. Benkirane, G. Guichard, J.-P. Briand, S. Muller, Exploration of requirements for peptidomimetic immune recognition. Antigenic and immunogenic properties of reduced peptide bond pseudopeptide analogues of a histone hexapeptide, J. Biol. Chem. 271 (1996) 33218–33224.

[6] F. Casset, F. Roux, P. Mouchet, C. Bès, T. Chardès, C. Granier, J.-C. Mani, M. Pugnière, D. Laune, B. Pau, M. Kaczorek, R. Lahana, A. Rees, A peptide mimetic of an anti-CD4 monoclonal antibody by rational design, Biochem. Biophys. Res. Commun. 307 (2003) 198–205.

[7] M.H. Van Regenmortel, S. Muller, D-peptides as immunogens and diagnostic reagents, Curr. Opin. Biotechnol. 9 (1998) 377–382.

[8] H.M. Dintzis, D.E. Symer, R.Z. Dintzis, L.E. Zawadzke, J.M. Berg, A comparison of the immunogenicity of a pair of enantiomeric proteins, Proteins 16 (1993) 306–308.

[9] A. Skerra, Engineered protein scaffolds for molecular recognition, J. Mol. Recogn. 13 (2000) 167–187.

[10] S.M. King, R.S. Patel-King, The M(r) = 8000 and 11,000 outer arm dynein light chains from *Chlamydomonas* flagella have cytoplasmic homologues, J. Biol. Chem. 270 (1995) 11445–11452.

[11] S.M. King, E. Barbarese, J.F. Dillman, R.S. Patel-King, J.H. Carson, K.K. Pfister, Brain cytoplasmic and flagellar outer arm dyneins share a highly conserved Mr 8,000 light chain, J. Biol. Chem. 271 (1996) 19358–19366.

[12] S.E. Benashski, A. Harrison, R.S. Patel-King, S.M. King, Dimerization of the highly conserved light chain shared by dynein and myosin V, J. Biol. Chem. 272 (1997) 20929–20935.

[13] F.S. Espindola, D.M. Suter, L.B. Partata, T. Cao, J.S. Wolenski, R.E. Cheney, S.M. King, M.S. Mooseker, The light chain composition of chicken brain myosin-Va: calmodulin, myosin-II essential light chains, and 8-kDa dynein light chain/PIN, Cell Motil. Cytoskeleton 47 (2000) 269–281.

[14] S.R. Jaffrey, S.H. Snyder, PIN: an associated protein inhibitor of neuronal nitric oxide synthase, Science 274 (1996) 774–777.

[15] A.D. Lajoix, R. Gross, C. Aknin, S. Dietz, C. Granier, D. Laune, Cellulose membrane supported peptide arrays for deciphering protein–protein interaction sites: the case of PIN, a protein with multiple natural partners, Mol. Divers. 8 (2004) 281–290.

[16] J. Liang, S.R. Jaffrey, W. Guo, S.H. Snyder, J. Clardy, Structure of the PIN/LC8 dimer with a bound peptide, Nat. Struct. Biol. 6 (1996) 735–740.
[17] H. Tochio, S. Ohki, Q. Zhang, M. Li, M. Zhang, Solution structure of a protein inhibitor of neuronal nitric oxide synthase, Nat. Struct. Biol. 5 (1998) 965–969.
[18] J. Fan, Q. Zhang, H. Tochio, M. Li, M. Zhang, Structural basis of diverse sequence-dependent target recognition by the 8 kDa dynein light chain, J. Mol. Biol. 306 (2001) 97–108.
[19] M.F. Krummel, M.M. Davis, Dynamics of the immunological synapse: finding, establishing and solidifying a connection, Curr. Opin. Immunol. 14 (2002) 66–74.
[20] L. Briant, C. Devaux, Bioactive CD4 ligands as pre and/or postbinding inhibitors of HIV-1, Adv. Pharmacol. 48 (2000) 373–407.
[21] C. Bès, M. Cerutti, L. Briant-Longuet, D. Bresson, S. Péraldi-Roux, M. Pugnière, J.-C. Mani, B. Pau, C. Devaux, C. Granier, G. Devauchelle, T. Chardès, The chimeric mouse-human anti-CD4 Fab 13B8.2 expressed in baculovirus inhibits both antigen presentation and HIV-1 promoter activation, Hum. Antibodies 10 (2001) 67–76.
[22] M. Benkirane, P. Corbeau, V. Housset, C. Devaux, An antibody that binds the immunoglobulin CDR3-like region of the CD4 molecule inhibits provirus transcription in HIV-infected T cells, EMBO J. 12 (1993) 4909–4921.
[23] S. Troadec, C. Bès, M. Chentouf, B. Nguyen, L. Briant, C. Jacquet, K. Chebli, M. Pugnière, F. Roquet, M. Cerutti, T. Chardès, Biological activities on T lymphocytes of a baculovirus-expressed chimeric recombinant IgG1 antibody with specificity for the CDR3-like loop on the D1 domain of the CD4 molecule, Clin. Immunol. 119 (2006) 38–50.
[24] D. Laune, F. Molina, G. Ferrieres, J.-C. Mani, P. Cohen, D. Simon, T. Bernardi, M. Piechaczyk, B. Pau, C. Granier, Systematic exploration of the antigen binding activity of synthetic peptides isolated from the variable regions of immunoglobulins, J. Biol. Chem. 272 (1997) 30937–30944.
[25] C. Monnet, D. Laune, J. Laroche-Traineau, M. Biard-Piechaczyk, L. Briant, C. Bès, M. Pugnière, J.-C. Mani, B. Pau, M. Cerutti, G. Devauchelle, C. Devaux, C. Granier, T. Chardès, Synthetic peptides derived from the variable regions of an anti-CD4 monoclonal antibody bind to CD4 and inhibit HIV-1 promoter activation in virus-infected cell, J. Biol. Chem. 274 (1999) 3789–3796.
[26] M. Pugnière, T. Chardès, C. Bès, C. Monnet, D. Laune, C. Granier, J.-C. Mani, Interaction analysis of CD4 with a synthetic peptide derived from the paratope of ST-40, an anti-CD4 monoclonal antibody, Int. J. Biochromatogr. 5 (2000) 187–197.
[27] R. Franck, Spot-synthesis : an easy technique for the positionally addressable, parallel chemical synthesis on a membrane support, Tetrahedron 98 (1992) 9217–9232.
[28] F. Molina, D. Laune, C. Gougat, B. Pau, C. Granier, Improved performances of spot multiple peptide synthesis, Pept. Res. 9 (1996) 151–155.
[29] C. Bès, L. Briant-Longuet, M. Cerutti, F. Heitz, S. Troadec, M. Pugnière, F. Roquet, F. Molina, F. Casset, D. Bresson, S. Péraldi-Roux, G. Devauchelle, C. Devaux, C. Granier, T. Chardès, Mapping the paratope of anti-CD4 recombinant Fab 13B8.2 by combining parallel peptide synthesis and site-directed mutagenesis, J. Biol. Chem. 278 (2003) 14265–14273.
[30] S.N. Ho, H.D. Hunt, R. Horton, J.K. Pullen, L. Pease, Site-directed mutagenesis by overlap extension using the polymerase chain reaction, Gene 77 (1989) 51–58.
[31] F. Manca, P. De Berardinis, D. Fenoglio, M.N. Ombra, G. Li Pira, D. Saverino, M. Autiero, L. Lozzi, L. Bracci, J. Guardiola, Antigenicity of HIV-derived T helper determinants in the context of carrier recombinant proteins: effect on T helper cell repertoire selection, Eur. J. Immunol. 26 (1996) 2461–2469.
[32] Y. Cheng, W.H. Prusoff, Relationship between the inhibition constant (K1) and the concentration of inhibitor which causes 50 percent inhibition (I50) of an enzymatic reaction, Biochem. Pharmacol. 22 (1973) 3099–3108.
[33] H.K. Binz, P. Amstutz, A. Plückthun, Engineering novel binding proteins from nonimmunoglobulin domains, Nat. Biotechnol. 23 (2005) 1257–1268.
[34] R.C. Ladner, Constrained peptides as binding entities, Trends Biotechnol. 13 (1995) 426–430.
[35] L.R. Helms, R. Wetzel, Proteolytic excision and in situ cyclization of a bioactive loop from an REI-VL presentation scaffold, Protein Sci. 3 (1994) 1108–1113.
[36] J. Janin, C. Chotia, The structure of protein–protein recognition sites, J. Biol. Chem. 265 (1990) 16027–16030.
[37] J.W. Smith, D. Hu, K. Satterthwait, S. Pinz-Sweeney, C.F. Barbas III, Building synthetic antibodies as adhesive ligands for integrins, J. Biol. Chem. 269 (1994) 32788–32795.
[38] E. Barbar, M. Hare, M. Makokha, G. Barany, C. Woodward, Dimerization and folding of LC8, a highly conserved light chain of cytoplasmic dynein, Biochemistry 40 (2001) 9734–9742.
[39] B. Peelle, J. Lorens, W. Li, J. Bogenberger, D.G. Payan, D.C. Anderson, Intracellular protein scaffold-mediated display of random peptide libraries for phenotypic screens in mammalian cells, Chem. Biol. 8 (2001) 521–534.
[40] D.A. Laplagne, V. Zylberman, N. Ainciart, M.W. Steward, E. Sciutto, C.A. Fossati, F.A. Goldbaum, Engineering of a polymeric bacterial protein as a scaffold for the multiple display of peptides, Proteins 57 (2004) 820–828.
[41] E.S. Ward, D. Güssow, A.D. Griffith, P.T. Jones, G. Winter, Binding activities of a repertoire of single immunoglobulin variable domains secreted from *Escherichia coli*, Nature 341 (1989) 544–546.
[42] B.L. Roberts, W. Markland, A.C. Ley, R.B. Kent, D.W. White, S.K. Guterman, R.C. Ladner, Directed evolution of a protein: selection of potent neutrophil elastase inhibitors displayed on M13 fusion phage, Proc. Natl. Acad. Sci. USA 89 (1992) 2429–2433.
[43] C.I. Wang, Q. Yang, S. Craik, Isolation of a high affinity inhibitor of urokinase-type plasminogen activator by phage display of ecotin, J. Biol. Chem. 270 (1995) 12250–12256.
[44] M. Uhlén, G. Forsberg, T. Moks, M. Hartmanis, B. Nilsson, Fusion proteins in biotechnology, Curr. Opin. Biotechnol. 3 (1992) 363–369.
[45] G. Beste, F.S. Schmidt, T. Stibora, A. Skerra, Small antibody-like proteins with prescribed ligand specificities derived from the lipocalin fold, Proc. Natl. Acad. Sci. USA 96 (1999) 1898–1903.
[46] D.L. Le Nguyen, A. Heitz, L. Chiche, B. Castro, R.A. Boigegrain, A. Favel, M.A. Coletti-Previero, Molecular recognition between serine proteases and new bioactive microproteins with a knotted structure, Biochimie 72 (1990) 431–435.
[47] C. Vita, J. Vizzavona, E. Drakopoulou, S. Zinn-Justin, B. Gilquin, A. Ménez, Novel miniproteins engineered by the transfer of active sites to small natural scaffolds, Biopolymers 47 (1998) 93–100.
[48] C. Vita, E. Drakopoulou, J. Vizzanova, S. Rochette, L. Martin, A. Ménez, C. Roumestand, Y.-S. Yang, L. Ylisastigui, A. Benjouad, J.-C. Gluckman, Rational engineering of a miniprotein that reproduces the core of the CD4 site interacting with HIV-1 envelope glycoprotein, Proc. Natl. Acad. Sci. USA 96 (1999) 13091–13096.
[49] Z. Lu, K.S. Murray, V. Van Cleave, E.R. LaVallie, M.L. Stahl, J.M. McCoy, Expression of thioredoxin random peptide libraries on the *Escherichia coli* cell surface as functional fusions to flagellin: a system designed for exploring protein–protein interactions, Bio/Technology 13 (1995) 366–372.
[50] G. Lee, W. Chan, M.R. Hurle, R.L. Desjalais, F. Watson, G.M. Sathe, R. Wetzel, Strong inhibition of fibrinogen binding to platelet receptor alpha IIb beta 3 by RGD sequences installed into a presentation scaffold, Protein Eng. 6 (1993) 745–754.
[51] B. Zhao, L.R. Helms, R.L. Desjalais, S.S. Abdel-Meguid, R. Wetzel, A paradigm for drug discovery using a conformation from the crystal structure of a presentation scaffold, Nat. Struct. Biol. 2 (1995) 1131–1137.